Pergamon

Int. J. Heat Mass Transfer. Vol. 39, No. 13, pp. 2791–2802, 1996

0017-9310/96 $15.00 + 0.00

0017-9310(95)00306-1

Heat transfer and fluid dynamics during the collision of a liquid droplet on a substrate—II. Experiments

Z. ZHAO and D. POULIKAKOS†

Mechanical Engineering Department, University of Illinois at Chicago, 842 W. Taylor Street, Chicago, IL 60680, U.S.A.

and

J. FUKAI

Chemical Engineering Department, Kyushu University, Fukuoka, 812, Japan

(*Received* 29 *November* 1994 *and in final form* 26 *July* 1995)

Abstract—This paper presents an experimental study of liquid droplet impingement upon a substrate. Qualitative as well as quantitative comparisons were conducted between the experimental measurements and the numerical predictions from the theoretical model in part 1 of this paper. The droplet deformation process was visualized using a two-reference-beam pulse holography method. Measurements of the transient splat radius were performed with a novel photoelectric technique. The experimentally obtained droplet shapes were similar to the numerically predicted ones for the same conditions. The impact dynamics was characterized by droplet spreading, recoiling and oscillations. The spreading and recoiling motions depended upon the initial velocity as well as the droplet properties. In summary, the theoretical predictions agreed well with the experimental results until the late stages of the droplet spreading process. Copyright © 1996 Elsevier Science Ltd.

1. INTRODUCTION

Experimental observations on the spreading of a liquid drop impacting on a flat surface have been reported in the literature as early as the late nineteenth century by Worthington [2, 3] who sketched artistically the various forms assumed by a droplet during its impact. For his observations, Worthington designed an ingenious inductor circuit which produced an electric spark for illumination at different stages of the droplet impact. More recently, a variety of high-speed photography techniques have been used to record the dynamic shapes of a droplet during the droplet/wall interaction [4–8]. These included the use of film camera, CCD video camera, and electronically controlled short-duration flash light photography. The clarity of pictures was greatly improved by using single-shot flash illumination [7, 8]. In a single-shot method only one image of a droplet is recorded at one instant of the impact process. By recording successive stages of the impact of several different drops the entire impact process can be pieced together from individual images [7]. Key parameters describing the droplet spreading process, i.e. splat/substrate contact area, splat diameter, splat thickness, etc., can be subsequently measured from the recorded splat pictures. The results reported in the aforementioned studies have improved our understanding of the complex fluid flow and heat transfer phenomena during the collision of a droplet on a solid surface.

An optical holography method was used in the present study to record the images in the droplet spreading process. The field distribution and phase information resulting from the light scattered by a deforming droplet was recorded on a hologram. The scattered field information recorded on a hologram provides a wealth of information about an object. For example, one hologram can readily generate different real images of a deforming splat that correspond to different viewing angles. The axial symmetry of a spreading drop can be examined for each exposure. In the present study, a two-reference-beam double-pulse holography system developed earlier [9–11] and available in our laboratory was used to study the droplet deformation. With this system, two holographic images of a droplet can be recorded and reconstructed from one hologram at two instances of the deformation process [9–11].

While visualization methods provide pictures of the splashing events at different stages, they have certain limitations. To exemplify, high-speed cine-

† Author to whom correspondence should be addressed. Current address: Institute of Energy Technology, Swiss Federal Institute of Technology, ETH Center, Sonneggstrasse 3, CH-8092, Zurich, Switzerland.

NOMENCLATURE

d_0	inital droplet diameter [m]	v_0	droplet impact velocity [m s^{-1}]
Fr	Froude number, $v_0^2/r_0 g$	We	Weber number, $\rho r_0 v_0^2/\gamma$.
g	gravitational acceleration [m s^{-2}]		
Pr	Prandtl number, ν/α	Greek symbols	
Pe	Peclet number, $r_0 v_0/\alpha$	α	thermal diffusivity [m^2 s^{-1}]
r_0	inital radius of droplet [m]	γ	surface tension coefficient [N m^{-1}]
R_{max}	dimensionless maximum radius of splat, r_{max}/r_0	μ	viscosity [kg s^{-1} m^{-1}]
Re	Reynolds number, $v_0 r_0/\nu$	ν	kinematic viscosity [m^2 s^{-1}]
t	time [s]	ρ	density [kg m^{-3}].

matography, in addition to being expensive to implement, can record multiple images of a single deforming droplet, but at the cost of reduction of image clarity, such that quantitative measurements are difficult. Single-shot flash photography can produce high clarity images of deforming droplets. However, only one image can be rendered for each impinging droplet. In general, visualization methods record deforming splat shapes at discrete stages of a continuous deformation process. Details of the entire droplet spreading and possibly recoiling process may be ignored due to insufficient information at certain stages. The splat size is usually measured from visualization images and the accuracy of the splat size measurements is of the order of 10 microns [7].

Efforts have been made to search for complementary experimental methods not involving direct visualization. Little progress has been made on this front since Shi and Chen [12] who measured the instantaneous radius of a spreading water droplet using an electrical resistance probe method [12]. In their experimental set-up, a glass plate was coated with a 10 μm thickness aluminum layer. A gap of 0.2 mm was scribed across the center separating the two halves of the conducting surface. An electrical d.c. voltage was applied to each half of the conducting surfaces. As a water droplet spreads at the center of the gap, the gap is bridged and the voltage across the gap decreases. By monitoring the voltage change across the gap, they were able to obtain the temporal change of splat radius. The calibration was performed by measuring the final 'disk' area vs the output signal voltage for impacting water droplets of known initial radiuses. While this method is of considerable merit, it has certain limitations. For example, different size droplets require different calibration curves. The recoiling of the splat can result in loss of data in high speed impact calibration. The 0.01 mm deep and 0.2 mm wide scribed channel is intrusive and could affect the spreading as well as the recoiling dynamics, especially for small size droplets. Finally, an off-center droplet spreading would result in experimental errors [12].

In the present study, a non-intrusive photoelectric method, was developed to measure the entire evolution of the maximum splat diameter during the collision of a droplet on a substrate. The time and length scales involved in this technique are of the order of microseconds and micrometers, respectively. The experimental setup of the photoelectric measurement system is described in detail in the present paper. The experimental results test the theoretical model reported in ref. [1].

2. EXPERIMENTAL PROCEDURES

The goals of the work are to validate the theoretical results in ref. [1] qualitatively and quantitatively and, in the process, to develop a non-intrusive and affordable method that can be used for the effective quantification of the droplet impinging process.

Since the main interest of the work is in liquid metal droplets, a liquid metal droplet generator (designed and fabricated in our laboratory) was utilized. This droplet generator performed two functions: first, it melted the metal under investigation and superheated the melt up to a desired temperature and, second, it generated one, or a sequence of liquid-metal droplets. The design details of the liquid metal droplet generator can be found in ref. [9, 13]. They are not repeated here for brevity. The ability of the droplet generator to produce liquid metal droplets with consistent size was tested by weighing the solidified splats. Figure 1 exemplifies the test results. The average droplet diameter and standard deviation are 2.96 and 0.013 mm respectively, for Group 1 and 2.99 and 0.034 mm respectively, for Group 2. Clearly, the performance of the liquid metal droplet generator is reliable.

Holography set-up for droplet spreading visualization

Optical holography was used to record the images of the deforming droplet at different stages of spreading. With the development of solid state pulsed laser equipment and modern electro-optic modulators, it is possible to freeze a deforming droplet within a very short time scale very reliably. To this end, a two-reference-beam holography system designed and tested along the lines described in refs. [9–11] was

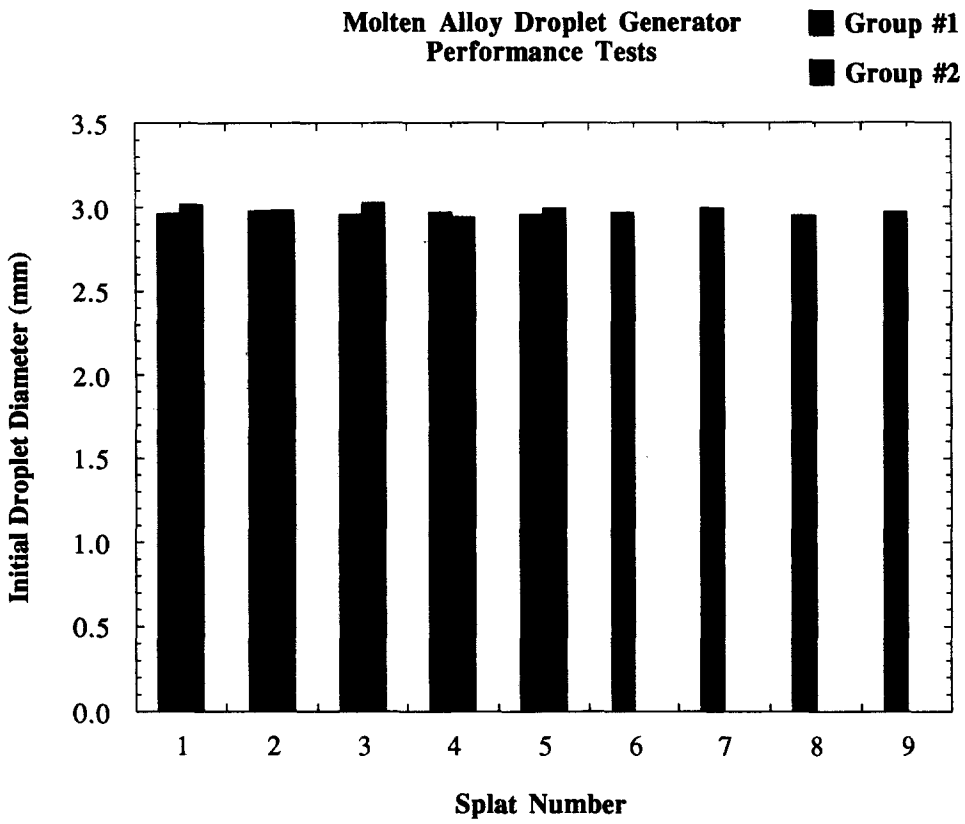

Fig. 1. Tests on the consistency of the liquid metal droplet generator.

utilized. Figure 2 shows the optical arrangement of the two-reference-beam holography image recording system. The key components in this arrangement are the Pockels cell and the polarizing beam splitter. During each experiment, the ruby laser fires two pulses of laser light ($\lambda = 694$ nm). The Pockels cell, driven by a high-voltage pulse generator, is electronically switched such that the polarization direction of the second pulse is rotated by 90°. This enables the second beam to pass through the polarizing beam splitter and follow the second reference path. Deforming droplet images from both the first and the second pulse are accordingly recorded on the same holographic plate, but with spatially different reference beams. In the present optical arrangement, the Pockels cell modulates both the object beam and the reference beam. This optical arrangement enables the polarization directions for the object beam and the reference beam to be used on the hologram plane. Therefore, a high degree of optical visibility is ensured for the holographic images recorded for both pulses. One reference beam at a time was used for reconstruction. Thus, two images of a splat at different stages of spreading can be separately reconstructed with exact information about the order [9–11]. The separation time between the first pulse image and the second pulse image is the same as the electronically set laser pulse separation time. The ruby laser used in this study was HLS-2 Ruby Laser by Lumonics Inc. The pulse duration was 20 ns and the pulse separation time varies in the range of 1 μs ~ 800 μs. The maximum laser beam power was 3 joules.

The overall setup for the droplet spreading experiments with holography is shown schematically in Fig. 3. A water-based ink (Permanent Black, Parker Pen USA Ltd) and fluxless solder were used for most of the experiments. The droplet is released from the droplet generator. It is detected by a droplet detector during its free-fall. After a preset time delay, the droplet detector sends a signal to trigger the pulse laser. The ruby pulse laser fires two pulses consecutively with a preset separation time and two images of a deforming droplet are recorded on the same holographic plate. The images are reconstructed from the holograms and digitized and stored in a personal computer (Macintosh Quadra 840) for image analysis (IMAGE ANALYST® version 8.0, 1992, Automatix, Inc).

A photoelectric technique for droplet spreading measurements

One of the objectives of the present study was to develop a fast, reliable and affordable measurement technique that is capable of recording the instantaneous splat diameter during its entire history non-intrusively. To this end, a photoelectric method was developed by utilizing a collimated laser beam and a linear response photodiode. Figure 4(a) shows schematically the optical layout of this measurement

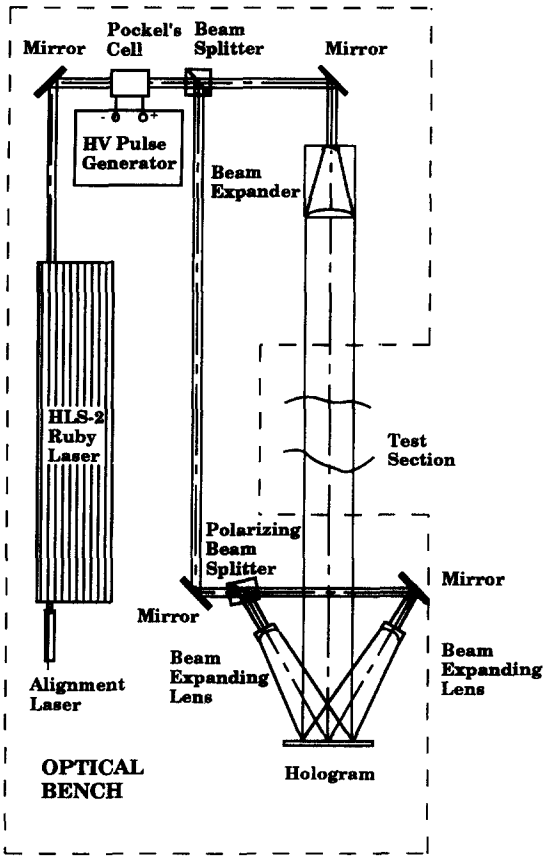

Fig. 2. Schematic of the two reference beam holography setup.

system. Its main principle is described as follows: as a droplet spreads out on a horizontal quartz plate, the splat area increases and consequently blocks increasingly more laser light. Therefore, the light intensity collected by the silicon photodiode decreases as the spreading proceeds. By recording the output signals from the Si-photodiode, the splat radius can be measured. The probe beam was provided by a 15 mW He-Ne laser ($\lambda = 632.8$ nm). The laser beam was focused and passed through a 20μm diameter spatial filter in order to produce a smooth irradiance across the expanded and collimated probe beam. An iris was used to improve the system sensitivity for small droplets. After intercepting the splat, the partially blocked beam was collected onto the sensor area of the Si-photodiode by a focusing lens. A silicon photodiode was chosen to detect the laser light because of its fast response and high linearity. The Si-photodiode used in this work was an E2RUV passive silicon photo detector (Photodiode type: S 1226-5BQ) manufactured by Spindler and Hoyer Inc. The photo detector rise time is 0.5 μs and the sensitive are a 2.4×2.4 mm^2. A 100-MHz oscilloscope (HP 54601A Oscilloscope, Hewlett-Packard Co.) recorded the output voltage signal. The angle between the probe beam axis and the vertical direction was $\theta = 8.5°$. The measurement system was calibrated by placing successively opaque circular disks of known area on the clear quartz to block the probe beam. The sample disks are precisely manufactured from a black cardboard using a computer operated CO_2 laser (C-80 Laser System, Laser Machining, Inc.). The system calibration curve is shown in Fig. 4(b). The calibration data points are represented by the circles. The solid line is a linear least-square fit of the calibration points. It is apparent that the system output signal is a linear function of the sample area. The uncertainty of the measurements obtained with this technique is directly related to the sensitivity of the oscilloscope and measurement system calibration. According to the calibration relation in Fig. 4(b) and sensitivity of the oscilloscope, the uncertainty of splat area measurements is less than 6.6×10^{-3} mm^2. This uncertainty of the splat area measurement results in uncertainties less than 2 μm and 1 μm for splat diameters larger than 2.1 and 4.2 mm, respectively.

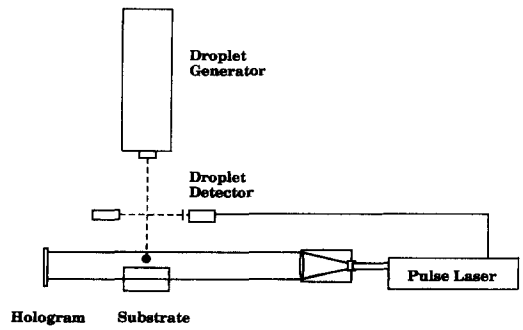

Fig. 3. Overall setup for droplet detection prior to impact on the substrate.

The current photoelectric method for the measurement of droplet spreading has limitations. For example, the droplet to be studied must be opaque to the probe beam. To alleviate this limitation, a special probe beam can be selected such that the droplet fluid is opaque to it. The probe beam wavelength is generally preferred to be in the range from visible to ultraviolet. Finally, a special wavelength window may be needed to reduce the environmental radiation that could affect the photoelectric measurements.

3. RESULTS AND COMPARISONS

A set of reconstructed images of an ink droplet splashing on a cubic quartz substrate, obtained with the holographic technique of the previous section, is shown in Fig. 5a, b. The droplet radius is 1.48 mm, and its impact velocity is 1.36 ms^{-1}. These conditions result in the following dimensionless numbers: $Re = 2000$, $We = 36$ and $Fr = 128$. Several observations on the droplet impact dynamics seen in the numerical results of ref. [1] are apparent in Fig. 5. First, the droplet liquid jets out radially from underneath the droplet. This jetting becomes visible at $t = 0.3$ ms after impact on the surface. The splat contour near the outer edge of the splat suggests that

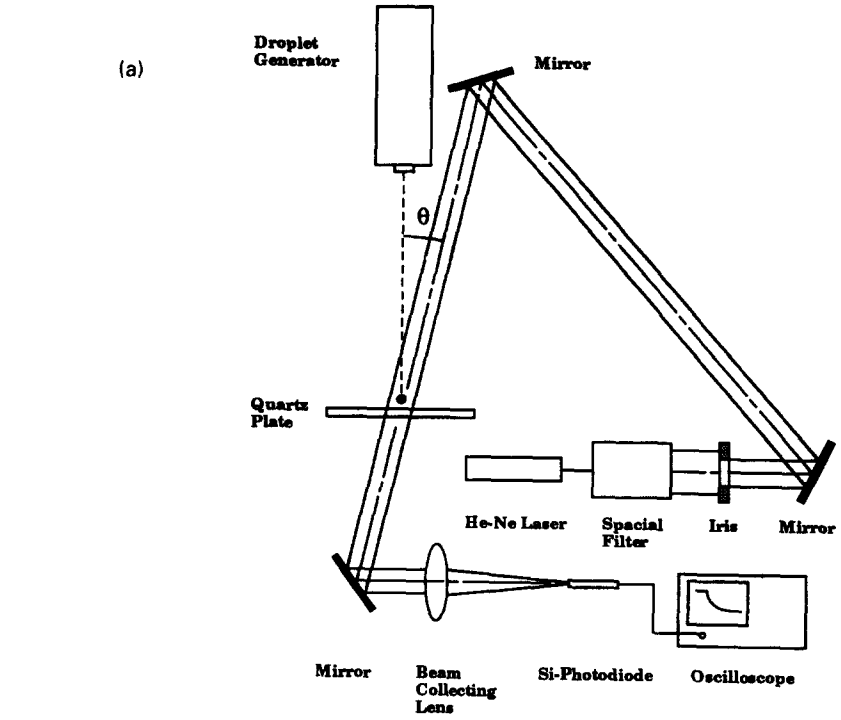

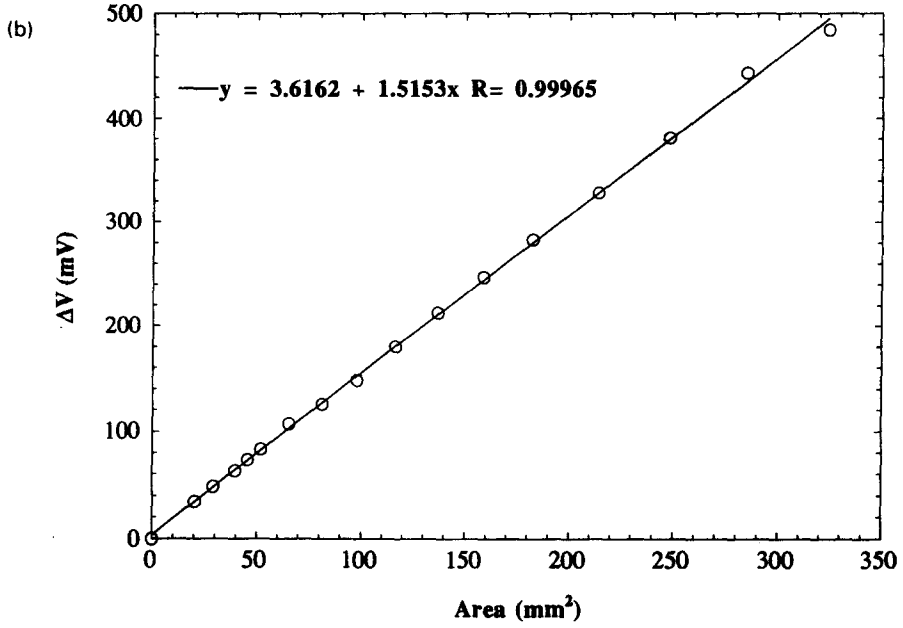

Fig. 4. (a) The photoelectric method for the measurement of splat diameter. (b) Calibration curve.

mass accumulation around the splat periphery starts as early as $t = 0.7$ ms. The ring structure around the splat periphery advanced radially and its height did not change appreciably during the spreading process (up to $t = 4.8$ ms). This finding agrees with the photographs by Chandra and Avedisian [7].

Direct photography methods usually record the splat image along with its reflection from the substrate. No reflection of the splat image exists in the holograms. In Fig. 5, the reconstructed image is 'projected' onto a two-dimensional plane (silhouette) which facilitates a direct comparison with numerical simulations under the same conditions. The holographic images at -0.3 ms and 0.1 ms correspond to the same deforming droplet. This is also true for the images at 0.7 ms and 1.1 ms.

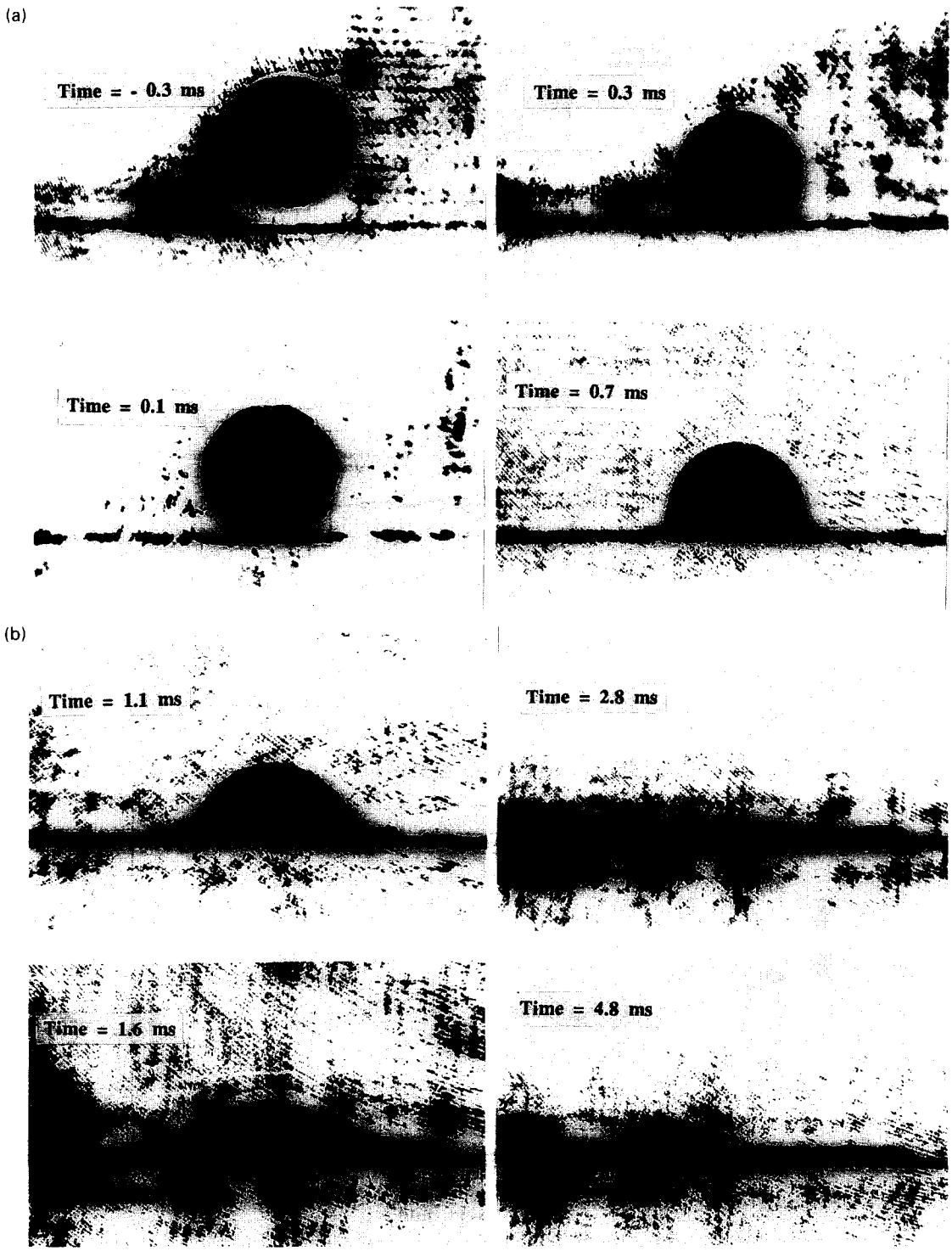

Fig. 5. Holography results for the spreading of an ink droplet on a substrate. (a) $t = -0.3$ ms to 0.7 ms. (b) $t = 1.1$ ms to 4.8 ms.

A numerical simulation under the same conditions as the above experiment was performed in ref. [1]. The numerical results are presented in Fig. 6. The length scale in Fig. 6 is normalized, based on the initial droplet radius, to facilitate the comparison with experimental results. The obvious similarity of splat shapes between Figs 5 and 6 at all spreading stages supports the results of ref. [1] for the highly complex flow field. The numerical simulations predict the major features of droplet impact dynamics correctly. Note that Fig. 6 shows a cross-section of the splat which makes the mass accumulation at the periphery more obvious

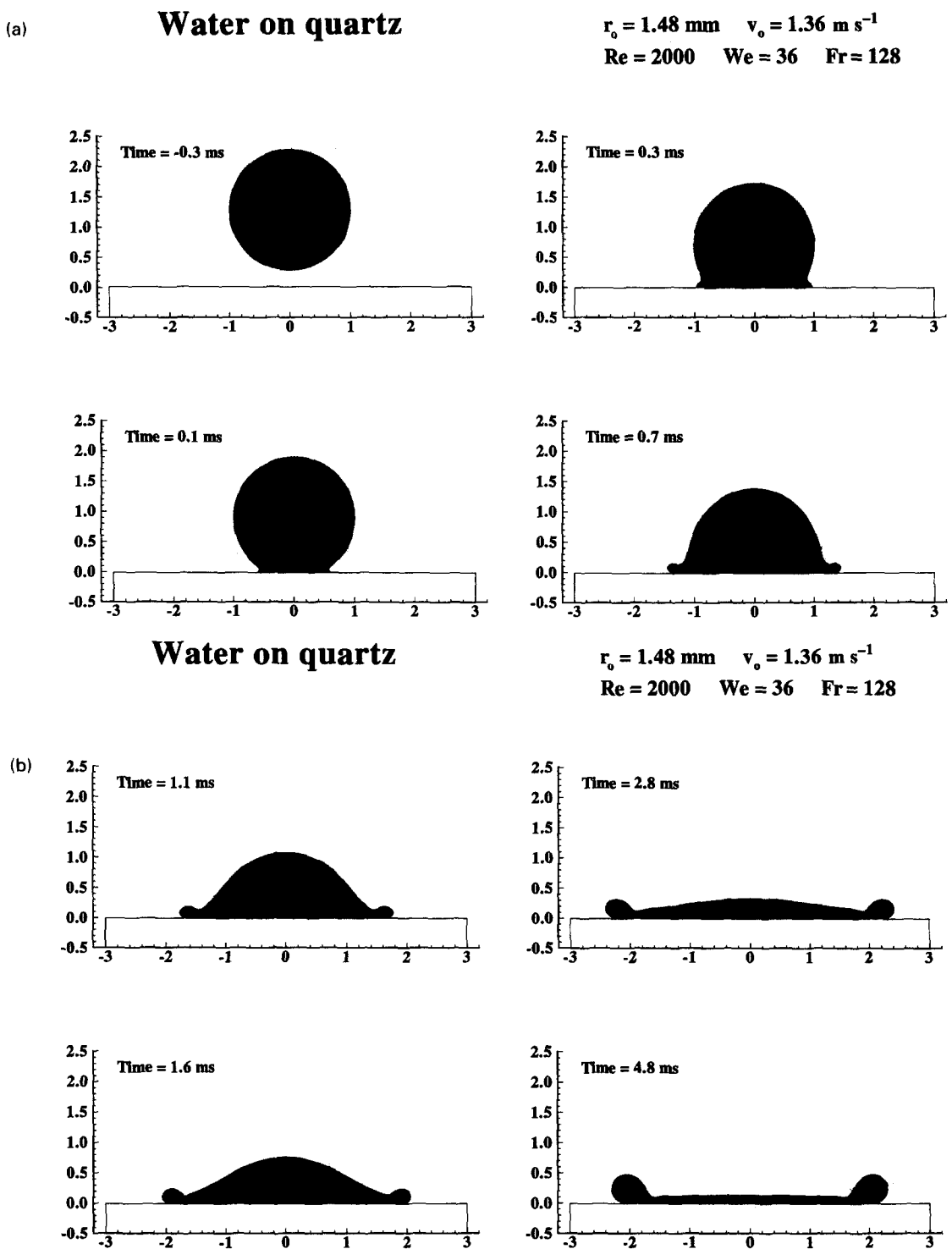

Fig. 6. Numerical simulation results for conditions identical to those of Fig. 5. (a) $t = -0.3$ ms to 0.7 ms. (b) $t = 1.1$ ms to 4.8 ms.

than in the front view photographs of Fig. 5. The slight difference between frames at 4.8 ms suggests that wetting effects at the moving contacting line become important at the late stages of spreading (prior to recoiling). The theoretical model of ref. [1] does not account for surface wetting at the moving contact line. Note that for the modeling of wetting, experimental results on the dynamic wetting angle (not available for the working fluids when this paper was written) need to be inputed to the theoretical model.

Quantitative measurements of instantaneous splat diameter were carried out with the photoelectric

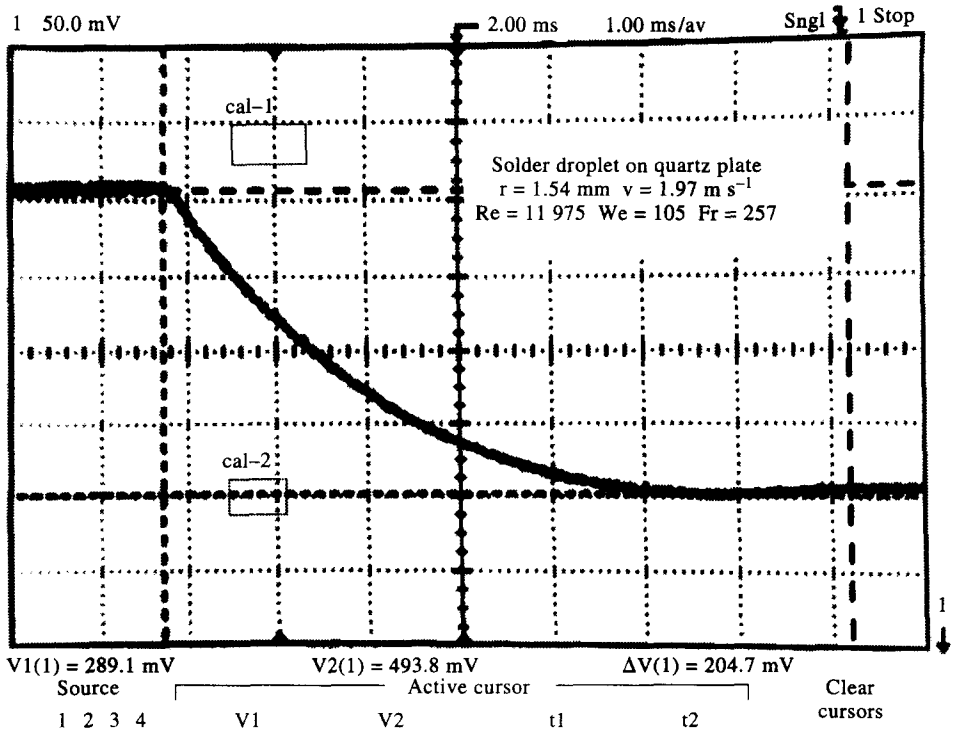

Fig. 7. Solder droplet spreading curve obtained with the photoelectric technique.

method explained in the previous section. An experiment was conducted by releasing a molten solder droplet with initial radius r_0 = 1.54 mm from a height of 198 mm onto a quartz plate. The resulted impact velocity was 1.97 m s^{-1}. Figure 7 shows the detected signal displayed on the oscilloscope. In Fig. 7, the horizontal axis represents the time with a unit of 1.0 ms per division; the vertical axis represents the output voltage with a unit of 50 mV per division. The experimental curve in Fig. 7 represents the temporal variation of the maximum splat radius. As the molten solder droplet collides with the solid surface and spreads outward, its maximum radius starts to grow, causing the incident light energy collected by the Si-photodiode to decrease. The spreading rate is higher during the initial stages (up to 2 ms) of impact. The spreading rate slows down and the radius finally reaches a maximum value. A slight splat recoiling was also recorded in Fig. 7 before the splat motion was completely halted by solidification.

In order to study further the impact dynamics of droplet spreading and recoiling, we conducted a series of experiments with the photoelectric method, using water based ink droplets. The ink fluid (Permanent Black, Parker Pen USA Ltd) was chosen because it is opaque to visible light. Ink droplets with radius r_0 = 1.48 mm are released from different heights and impact on a quartz plate. In order to limit wetting and enhance recoiling, the quartz plate was coated with a non-wetting layer, Rain-X (Unelko Co., USA). The coating layer was dried before conducting the experiments.

The impact histories of different events recorded on the oscilloscope are shown in Fig. 8a–d. The two curves in Fig. 8b represent the peak and the valley values of the same signal at the same instance. The measurements are based on the difference between the initial signal value and the signal values during spreading (the absolute value of the signal is not used). Therefore, any two of the curves can be utilized for measurements. Since the peak signal has less random noise, it was utilized throughout the experiments. Figure 8a depicts the impact history of an ink droplet with radius r_0 = 148 mm released from a height of 205mm. The droplet impacts on the quartz plate and quickly spreads out. After the splat reaches a maximum value, it gradually recoils. The curve finally reaches a plateau. The difference between the initial value of the value of output voltage signal and the final value indicates that the radius of the splat at the rest state is larger than the initial droplet radius. The spreading and recoiling process of the ink droplet released from a lower height, 155 mm, is recorded in Fig. 8b. Figure 8b shows that the droplet spreads to a maximum splat area in about 4.5 ms and subsequently recoils. The first recoiling lasts about 30.5 ms. After recoiling the splat spreads again and finally recoils to the rest state. The magnitude of the second spreading and recoiling events are smaller compared with the first spreading and recoiling events. In Fig. 8c, the ink droplet is released from a 50 mm height. It is immediately apparent that the splat radius at the end of the first recoiling event reaches approximately the same value as the droplet initial radius. The spreading

and recoiling dynamics of the droplets for an even smaller droplet release height of 33 mm is shown in Fig. 8d. The first recoiling yields a state where the resulting splat radius becomes smaller than the initial droplet radius.

It is evident from Fig. 8a–d that the magnitudes of the droplet first spreading and recoiling events (change of splat radius) are substantially larger than the oscillatory motion thereafter. This result suggests that, within the impact velocity range of this study,

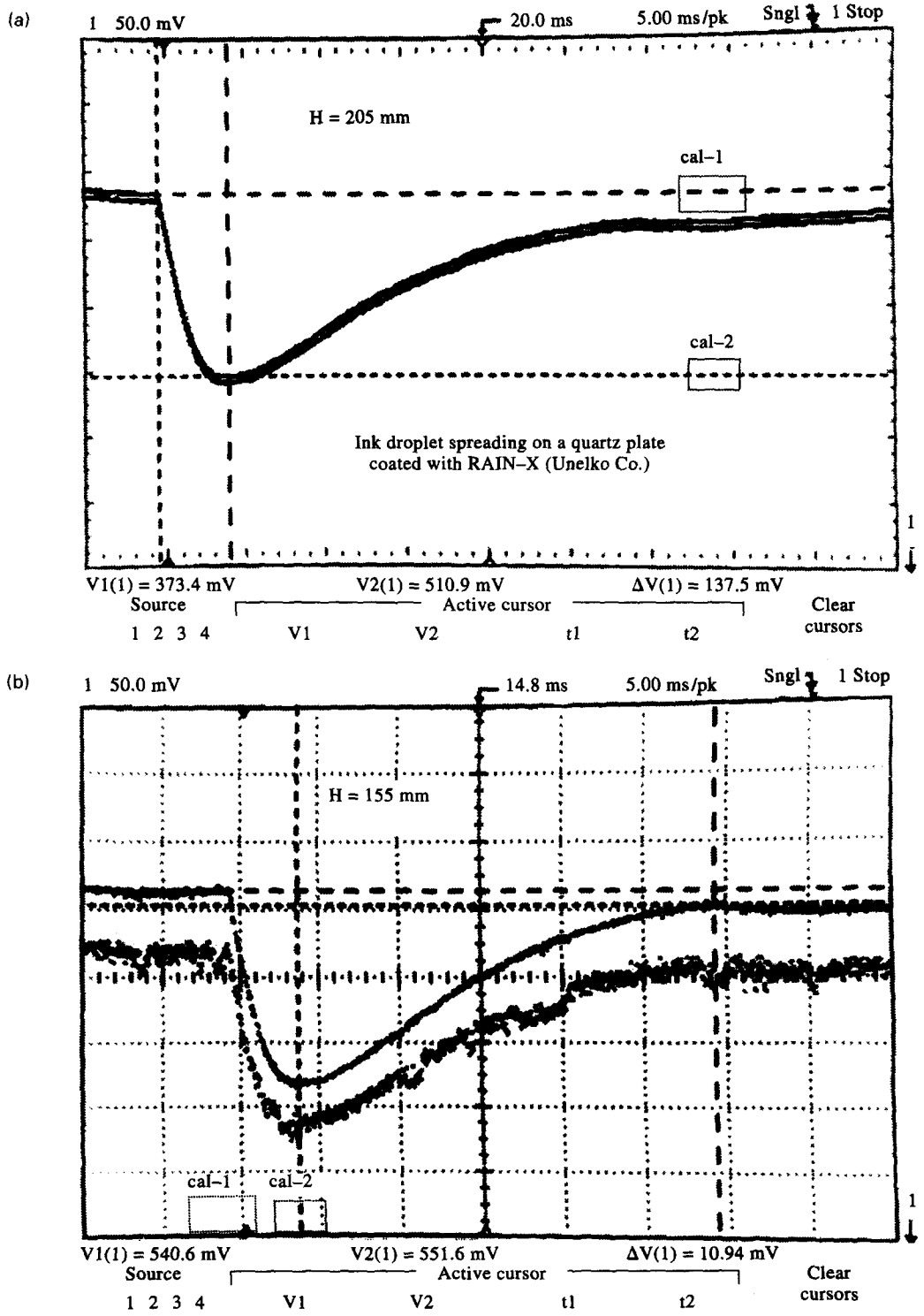

Fig. 8. Variation voltage output with time illustrating the ink droplet results obtained with the photoelectric technique. (a) Droplet release distance 205 mm. (b) Droplet release distance 155 mm. (c) Droplet release distance 50 mm. (d) Droplet release distance 33 mm. (*Continued overleaf.*)

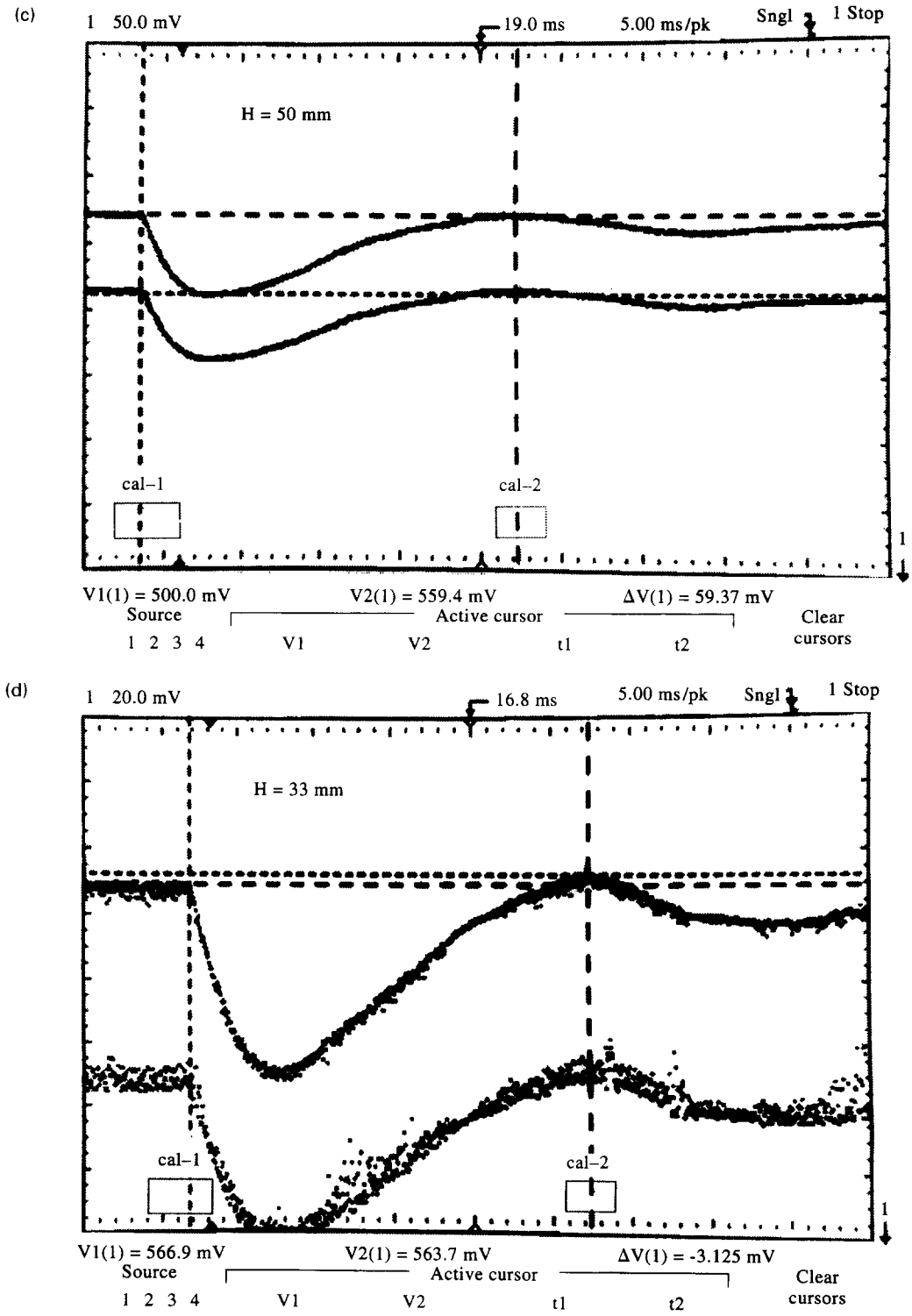

Fig. 8. *Continued.*

the droplet impact energy is dissipated primarily within the first cycle of droplet spreading and recoiling. The first recoiling lasts longer than the first spreading, Fig. 8a–d. This is due to the combined effects of droplet energy dissipation and contact angle hysteresis (the contact angle adjusts from its spreading to its recoiling value when the splat is fully spread). During the first spreading motion, the fluid flow was inertia dominated (at the impact speeds of the current studies). Part of the kinetic energy is stored as surface tension potential energy and part is dissipated into viscous energy by the end of the first spreading

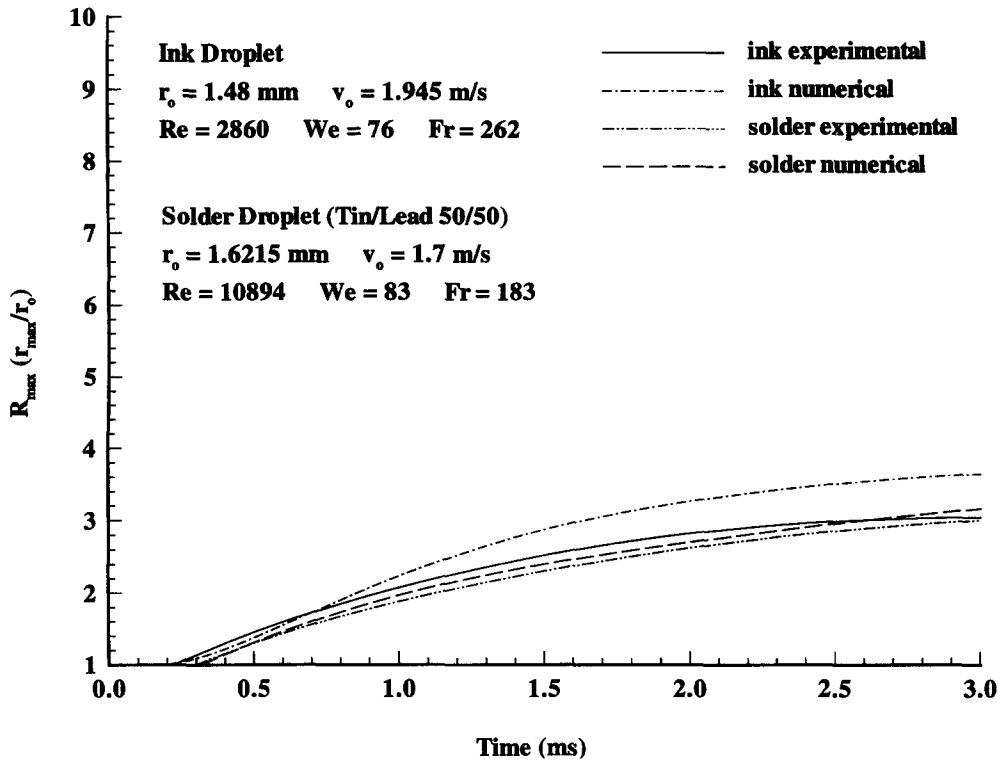

Fig. 9. Comparison of theoretical and experimental results on the maximum splat radius.

motion. Hence, the surface tension potential energy stored in the deforming splat just prior to recoiling is smaller than the initial impact energy. Therefore, the recoiling speed is smaller than the spreading speed and the recoiling time is longer than the spreading time. The droplet fluid flow is surface tension dominated after the first spreading. The advancing contact angle is generally larger than the droplet recoiling contact angle. Therefore, the impeding effects of capillary forces on the movement of the contact line is stronger during droplet recoiling, which further reduces the speed of receding motion.

The theroetical model of ref. [1] was quantitatively validated by performing numerical simulations under the same conditions as in the experimental investigations with the photoelectric technique. The variation of the maximum splat ratio measured with the photoelectric method was compared with the numerical predictions. Representative results of such comparisons are shown in Fig. 9. In the case of the ink droplet, the numerical predictions of the temporal variation of the maximum splat radius are close to the measurements in the early stages of spreading. The difference between numerical simulations and experiments gradually increases as the spreading proceeds because the wetting effects at the moving contact line are becoming increasingly important as the inertial forces are gradually reduced. In any event, the maximum difference between experiments and numerical predictions occurring at the end of the spreading process is less than 18%. The agreement between theory and experiment is considerably improved in the case of the liquid solder droplet. This is due to the fact that wetting effects are not as important in this case because liquid solder wets the glass surface markedly less than water based ink.

4. CONCLUSIONS

This paper presented an experimental study of droplet impingement upon a substrate prior to the onset of solidification. The experimental investigation of the droplet impact dynamics was accomplished with a two-reference-beam holography method for the visualization of the droplet deformation and with of a novel photoelectric technique for the fast recording of the splat radius during spreading and recoiling on a flat surface. The experimental results were used to validate the theoretical model of ref. [1], both qualitatively and quantitatively.

A two-reference-beam holography system was used to visualize droplet spreading. The experimentally recorded splat shape at different stages of the spreading shows marked similarity with the numerical predictions, underpinning the reliability of the numerical modeling. A simple and accurate non-intrusive technique was presented for the measurement of the transient splat radius. The results showed that the fluid motion in the droplet first spreading and recoiling cycle is substantially stronger than that in subsequent cycles or oscillations. This finding suggests that, within the impact velocity range of this study, most

of the droplet impact energy is dissipated within the first cycle of droplet spreading and recoiling. In addition, in this first cycle, the duration of the spreading motion was considerably shorter than the duration of the recoiling motion. Quantitative comparisons between numerical simulations and experimental measurements for the transient splat radius showed good agreement, better at the earlier stages of the spreading process.

REFERENCES

1. Z. Zhao, D. Poulikakos and J. Fukai, Heat transfer and fluid dynamics during the collision of a liquid droplet on a substrate—I. Modeling *Int. J. Heat Mass Transfer* **39,** 2771–2789 (1996).
2. A. M. Worthington, On the forms assumed by drops of liquid falling on a horizontal plate, *Proc. R. Soc. Lond.* **25,** 261–271 (1877)
3. A. M. Worthington, A second paper on the forms assumed by drops of liquids falling vertically on a horizontal plate, *Proc. R. Soc. Lond.* **25,** 498–503 (1877)
4. O. G. Engel, Waterdrop collision with solid surfaces, *J. Res. Natl Bureau Standards* **54,** 281–298 (1955)
5. L. H. Wachters and N. A. Westerling, The heat transfer from a hot wall to impinging water drops in the spherical state, *Chem. Engng Sci.* **21,** 1047–1056 (1966).
6. S. Toda, A study of mist cooling (2nd report : Theory of mist cooling and its fundamental experiments), *Heat Transfer Jap. Res.* **1,** 1–44 (1974)
7. S. Chandra and C. T. Avedisian, On the collision of a droplet with a solid surface. *Proc. R. Soc. Lond. A* **432,** 13–41 (1991).
8. A. L. Yarin and D. A. Weiss, Impact of drops on solid surfaces : self-similar capillary waves, and splashing as a new type of kinetic discontinuity. *J. Fluid Mech.* **283,** 141–173 (1995).
9. Z. Zhao, Transport phenomena during the impingement of liquid-metal droplets on a substrate, Ph.D. Thesis, University of Illinois at Chicago (1994)
10. B. Kang, A holographic study of the dense spray region created by two-impinging jets, Ph.D. Thesis, The University of Illinois at Chicago (1995).
11. B. Kang, D. Poulikakos and Y. Shen, Holography experiments in the breakup region of a liquid sheet formed by two impinging jets, *Atomization Sprays* **5,** 387–402 (1995).
12. M. H. Shi and J. C. Chen, Behavior of a liquid droplet impinging on a solid surface. *The American Society of Mechanical Engineers*, 83-WA/HT-104 (1983).
13. B. Kang. Z. Zhao and D. Poulikakos, Solidification of liquid-metal droplets impacting sequentially on a solid surface. *J. Heat Transfer* **116,** 436–445 (1994).